

Direct brain recordings reveal occipital cortex involvement in memory development

Qin Yin^{a,b}, Elizabeth L. Johnson^{a,c}, Lingfei Tang^{a,b}, Kurtis I. Auguste^{d,e}, Robert T. Knight^{c,f}, Eishi Asano^g, Noa Ofen^{a,b,*}

^a Life-Span Cognitive Neuroscience Program, Institute of Gerontology and Merrill Palmer Skillman Institute, Wayne State University, Detroit, MI, USA

^b Department of Psychology, Wayne State University, Detroit, MI, USA

^c Helen Wills Neuroscience Institute, University of California, Berkeley, CA, USA

^d Department of Neurological Surgery, University of California, San Francisco, CA, USA

^e Department of Surgery, Division of Neurological Surgery, Children's Hospital and Research Center, Oakland, CA, USA

^f Department of Psychology, University of California, Berkeley, CA, USA

^g Departments of Pediatrics and Neurology, Children's Hospital of Michigan, Wayne State University, Detroit, MI, USA

ARTICLE INFO

Keywords:

Visual memory
Occipital cortex
Electrocorticography
Alpha oscillations
Memory development
Scene complexity

ABSTRACT

Processing of low-level visual information shows robust developmental gains through childhood and adolescence. However, it is unknown whether low-level visual processing in the occipital cortex supports age-related gains in memory for complex visual stimuli. Here, we examined occipital alpha activity during visual scene encoding in 24 children and adolescents, aged 6.2–20.5 years, who performed a subsequent memory task while undergoing electrocorticographic recording. Scenes were classified as high- or low-complexity by the number of unique object categories depicted. We found that recognition of high-complexity, but not low-complexity, scenes increased with age. Age was associated with decreased alpha power and increased instantaneous alpha frequency during the encoding of subsequently recognized high- compared to low-complexity scenes. Critically, decreased alpha power predicted improved recognition of high-complexity scenes in adolescents. These findings demonstrate how the functional maturation of the occipital cortex supports the development of memory for complex visual scenes.

1. Introduction

Our ability to remember complex visual stimuli shows robust gains from childhood through young adulthood. Research on the neural basis of these age-related gains in memory has primarily focused on the protracted maturation of brain regions identified as crucial for memory, such as the prefrontal cortex and medial temporal lobe (Johnson et al., 2018; Ofen, 2012; Ofen et al., 2019, 2007; Tang et al., 2018; Yu et al., 2018). Yet, several lines of work point to the critical role of visual processing in the development of memory, and thus the protracted maturation of brain regions involved in visual processing as a key factor in limiting young children's memory for visual stimuli (Chai et al., 2010; Golarai et al., 2010, 2007; Gomez et al., 2017). Evidence of the protracted development of basic aspects of visual processing (van den Boomen, van der Smagt and Kemner, 2012), combined with structural

changes in the occipital cortex (Ducharme et al., 2016; Huttenlocher et al., 1982), raises the possibility that the functional maturation of the occipital cortex plays an important role in visual memory development. Here, we provide direct evidence recorded from the occipital cortex in children and adolescents demonstrating the involvement of the occipital cortex in memory formation across development.

Functional and structural MRI studies have documented the protracted maturation of category-selective, high-level visual regions such as the ventral temporal cortex (Golarai et al., 2010; Gomez et al., 2018, 2017; Natu et al., 2019; Peelen et al., 2009; Scherf et al., 2007). The maturation of these category selective high-level visual regions is associated with developmental gains in recognition memory for scenes and faces (Chai et al., 2010; Golarai et al., 2010, 2007; Gomez et al., 2017), suggesting a link between the maturation of high-level visual processes and the development of visual memory.

* Corresponding author. Life-Span Cognitive Neuroscience Program, Institute of Gerontology and Merrill Palmer Skillman Institute, Wayne State University, Detroit, MI, USA.

E-mail address: noa.ofen@wayne.edu (N. Ofen).

<https://doi.org/10.1016/j.neuropsychologia.2020.107625>

Received 1 March 2020; Received in revised form 25 July 2020; Accepted 9 September 2020

Available online 15 September 2020

0028-3932/© 2020 Elsevier Ltd. All rights reserved.

Studies of behavior and visual evoked potentials have also identified prolonged maturation of several aspects of visual processing which constitute the basic building blocks of scene perception (van den Boomen, van der Smagt and Kemner, 2012). Evidence of prolonged maturation comes from studies of contrast sensitivity during the perception of natural images, with differences observed between children aged 6–10 years and adults (Ellemberg et al., 2012), and between children and adolescents aged 7–15 years and adults (Rokszin et al., 2018). Prolonged maturation was further documented in study of spatio-chromatic processing, with age differences observed in participants aged 2–26 years (Madrid and Crognale, 2000). There is also evidence of age differences

in orientation perception as indexed by texture segregation between infants, 13-year-olds, and adults (Sireteane and Rieth, 1992), and as indexed by spatial integration between participants aged 5–14 years and adults (Kovacs et al., 1999). Finally, there is evidence of age differences in stereoacuity between children aged 5–10 years and adults (Sloper and Collins, 1998). Collectively, these studies point to the prolonged development of low-level visual processes. Evidence that basic, low-level aspects of visual processing continue to develop throughout childhood and adolescence is consistent with the notion of prolonged functional development of the human visual system.

The prolonged development of low-level visual processes is further

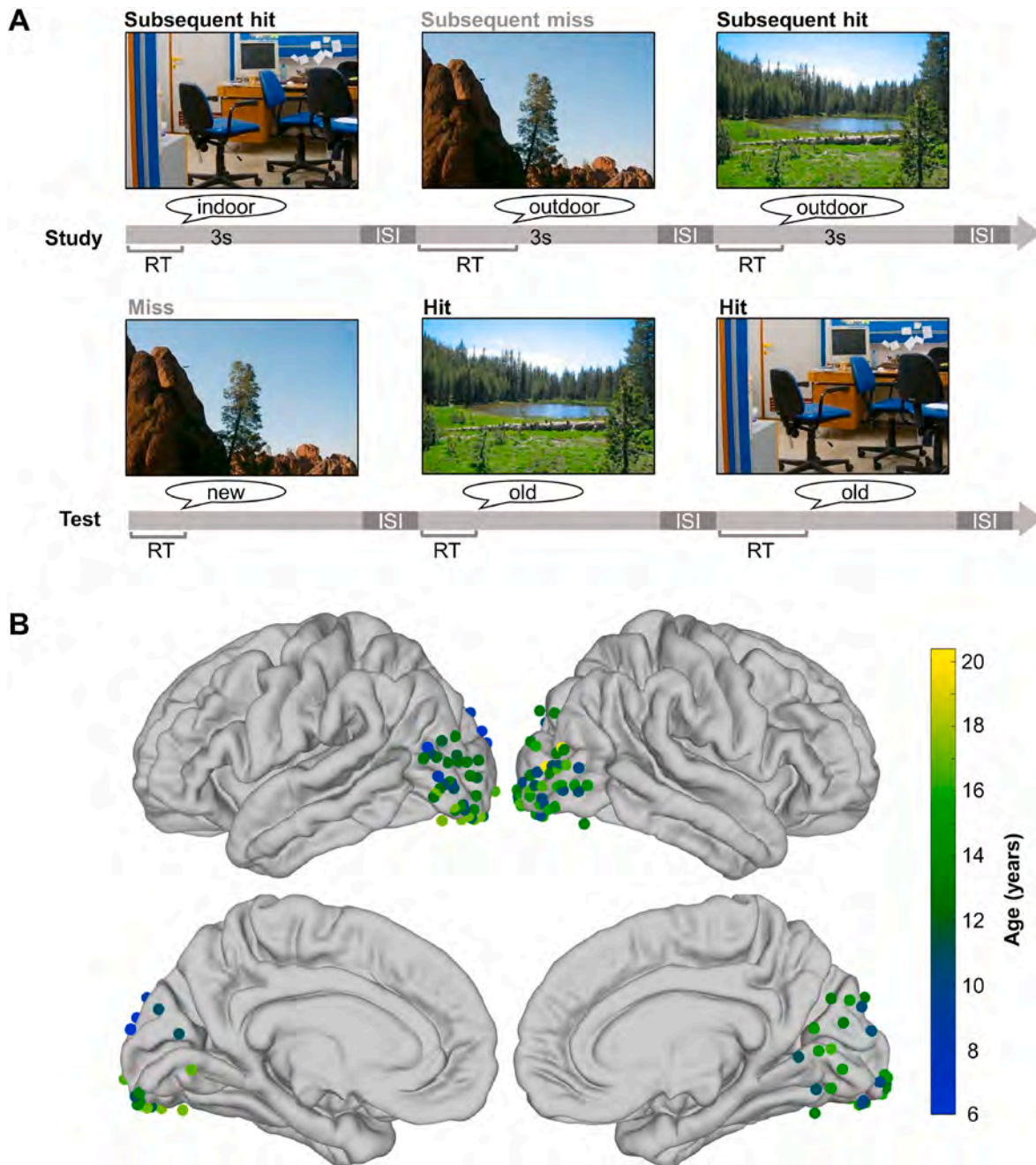


Fig. 1. Scene subsequent memory paradigm and electrode coverage. (A) Subsequent memory paradigm. Scenes were presented in two consecutive study-test cycles. In each study cycle, participants studied 40 scenes (3000 ms each) and indicated whether each scene was indoor/outdoor. In each test cycle, participants were tested on all 40 studied scenes, intermixed with 20 new scenes as foils. Participants made an old/new judgement of each scene based on whether they remembered seeing the scene at study. The test was self-paced. ISI, interstimulus interval (500 ms fixation). (B) Reconstruction of occipital cortex electrode coverage ($n = 109$) for all participants ($n = 24$). Each electrode was color-coded by participant's age. (For interpretation of the references to color in this figure legend, the reader is referred to the Web version of this article.)

supported by evidence of the prolonged structural maturation of the occipital cortex. Neuroimaging anatomical evidence shows that the occipital cortex continues to mature through adolescence, as evident in age differences in cortical thickness in participants aged 5–21 years (Ducharme et al., 2016), suggesting synaptic pruning of inefficient connections as observed in brains varying in age from fetal gestation week 28 to 71 years (Huttenlocher et al., 1982). Given that memory for visual stimuli depends on input from the occipital cortex, these findings raise the possibility that the maturation of the occipital cortex contributes to the development of memory for complex visual stimuli. Overall, evidence suggests that *the functional maturation of the occipital cortex may be critical for developmental gains in perception and therefore also in memory.*

To test this proposal, we capitalized on a rare opportunity to investigate activity recorded directly from the occipital cortex in 24 children and adolescents who performed a subsequent memory task while undergoing electrocorticographic (ECoG) recording (Fig. 1). ECoG data provide unprecedented spatiotemporal resolution in the study of neurocognitive development (Ofen et al., 2019), and coverage of the occipital cortex is exceedingly rare (Parvizi and Kastner, 2018). To assess differences in visual processing, we took advantage of scene complexity. All scenes were of either high or low complexity, defined by the number of unique object categories depicted (Fig. 2A). We investigated visual processing by analyzing the difference in occipital ECoG signals during the encoding of high- compared to low-complexity scenes (Chai et al., 2010; Russell et al., 2008). We further investigated how visual processing contributed to memory formation by comparing effects during the perception of scenes that were subsequently recognized correctly or forgotten (Ofen et al., 2019). We focused on oscillations in the alpha range (~7–14 Hz) given the well-established role of alpha oscillations in visual processing (for a review, see Clayton, Yeung and Cohen Kadosh, 2017). We measured two aspects of alpha oscillations: broadband power and instantaneous frequency.

Decreased alpha power has been proposed to reflect increased neural activity, as demonstrated by inverse relationships between alpha power and multiunit neuronal activity (Haegens et al., 2011; van Kerkoerle et al., 2014) and hemodynamic fMRI responses (Goldman et al., 2002; Harvey et al., 2013). More recently, alpha power decreases have been termed alpha *desynchronization*, which has been proposed to index the richness of information encoded by the brain, and more specifically to predict memory encoding success (Hanslmayr et al., 2016, 2012). Indeed, alpha desynchronization is associated with subsequent memory formation (Griffiths et al., 2019; Johnson et al., 2020; Lega et al., 2017).

Time-resolved peak alpha frequency has been proposed to modulate the timing of neuronal spiking (Cohen, 2014) and support rhythmic perception (Samaha and Postle, 2015; VanRullen, 2016). Electrophysiological evidence suggests that visual perception happens in a cyclic manner such that particular phases of the alpha cycle are associated with increased neural activity (Haegens et al., 2011; Klimesch et al., 2007) and thus more efficient sensory perception than others (Busch et al., 2009; Busch and VanRullen, 2010; Mathewson et al., 2009). Therefore, time-resolved peak alpha frequency, measured here by instantaneous frequency (Cohen, 2014), may index the temporal resolution of perception (Samaha and Postle, 2015; Shen et al., 2019; Wutz et al., 2018).

Alpha power and instantaneous frequency are thought to reflect the dynamics of neural activity which regulate visual information processing (Nelli et al., 2017). Therefore, we hypothesized that measures of alpha power and frequency would reveal complementary age-related differences in the processing of complex visual scenes. In addition, alpha power and instantaneous frequency may reflect dissociable properties of visual information processing. Whereas broadband alpha power may reflect the rate of neuronal spiking and predict memory outcomes (Hanslmayr et al., 2016, 2012), instantaneous alpha frequency may reflect the timing of neuronal spiking and predict perceptual outcomes (Cohen, 2014; Samaha; Postle, 2015; Shen et al., 2019; Wutz et al., 2018). Thus, we anticipated that alpha power and frequency would show complementary but dissociable relationships with memory performance.

Using the same scene subsequent memory paradigm (Fig. 1A), Chai et al. (2010) previously found age-related improvements in the recognition of high- but not low-complexity scenes. These improvements in high-complexity scene recognition accuracy were associated with the functional maturation of the parahippocampal gyrus, as measured by fMRI during scene encoding. They also found that viewing high-complexity scenes induced greater activation in the occipital cortex compared to low-complexity scenes, suggesting that the perception of complex scenes demands low-level visual processes. Here, we hypothesized that age-related differences in occipital alpha power and frequency would be specific to the perception of high-complexity scenes that were subsequently recognized. We further tested the extent to which these age differences would predict age-related improvements in the recognition of complex visual scenes, thus linking the maturation of low-level visual processes to developmental gains in memory for complex visual scenes.

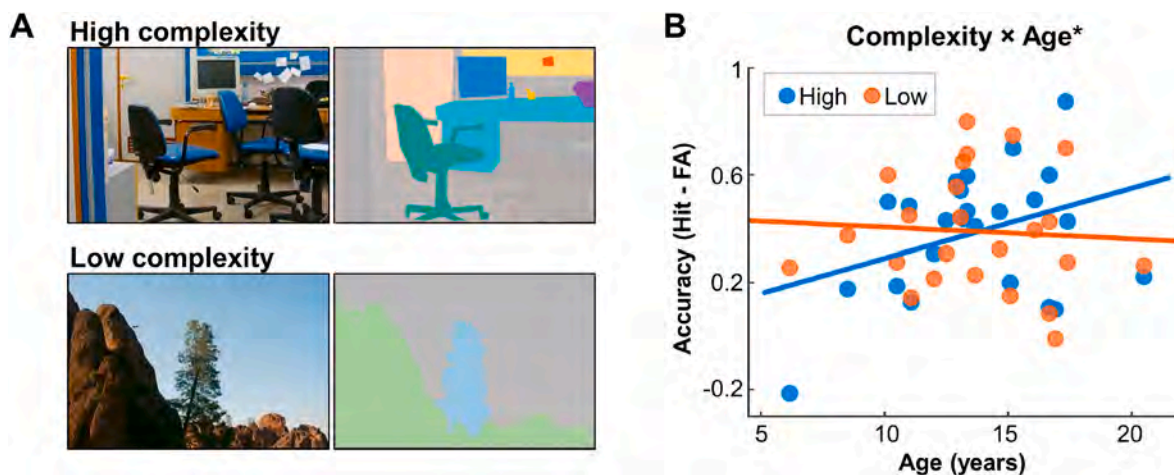


Fig. 2. Age-related increase in recognition of high- but not low-complexity scenes. (A) Examples of high-complexity (top; defined by 5 or more object categories) and low-complexity (bottom; 3 or fewer object categories) scenes. Original scenes are presented on the left and object categories identified in those scenes are presented on the right, indicated by different colors. (B) There was an age by scene complexity interaction in recognition accuracy (hit rate – false alarm [FA] rate; $p < 0.001$). The interaction was driven by an age-related increase in the recognition of high- (blue; $p = 0.09$; $r = 0.36$) but not low-complexity (orange; $p = 0.77$; $r = -0.06$) scenes. (For interpretation of the references to color in this figure legend, the reader is referred to the Web version of this article.)

2. Materials and methods

2.1. Participants

Twenty-six neurosurgical patients (15 males; 6.2–20.5 years of age; mean \pm SD, 13.6 ± 3.3 years) with subdural electrodes implanted for the clinical evaluation of refractory epilepsy participated in this study. Twenty-five patients were from the Children's Hospital of Michigan, and one patient was from the University of California, San Francisco, Benioff Children's Hospital. Written informed consent was obtained from patients aged 18 years and older and from the guardians of participants under age 18 years. Written assent was obtained from participants aged 13–17 years and oral assent was obtained from younger children. This study was approved by the Institutional Review Board at each data collection site in accordance with the Declaration of Helsinki. Data from two participants were excluded from analysis due to overall negative recognition accuracy (age 9.3 years, accuracy = -0.14 ; age 16.7 years, accuracy = -0.06), resulting in 24 participants (13 males; 6.2–20.5 years of age; mean \pm SD, 13.7 ± 3.2 years; Table S1).

2.2. Stimuli

A total of 120 full-color pictures of natural scenes (60 indoor, 60 outdoor) were used in the subsequent memory paradigm (Fig. 1A). Pictures of scenes were classified as high- or low-complexity by the number of unique object categories depicted (Fig. 2A), as determined using the LabelMe image toolbox (Russell et al., 2008). Scenes that included five or more object categories were classified as high-complexity, and scenes that included three or fewer object categories were classified as low-complexity (Chai et al., 2010). High- and low-complexity scenes were fully counter-balanced within each of the study and test cycles, as described below. The spatial frequency of each scene was characterized and compared between high- and low-complexity scenes using the method of Chai et al. (2010). There was no difference between high- and low-complexity scenes in spatial frequency ($t_{(118)} = 0.95$, $p = 0.34$).

2.3. Subsequent memory task

Memory formation was assessed in a scene subsequent memory paradigm (Fig. 1A) that has been used extensively in this age group (Chai et al., 2010; Johnson et al., 2018; Ofen et al., 2019, 2007; Tang et al., 2018). Scenes were presented in two consecutive study-test cycles. In each study cycle, participants studied 40 scenes (20 indoor, 20 outdoor), each presented for 3000 ms following a 500-ms fixation screen. Participants verbalized whether each scene was "indoor" or "outdoor" in preparation for a recognition test. Responses were coded as correct or incorrect via offline review of individual audio recordings. Analysis of electrophysiological data was restricted to studied scenes that were properly attended, as indicated by a correct indoor/outdoor response.

In each test cycle, participants were tested on all 40 studied scenes, intermixed with 20 new scenes as foils. Participants were instructed to respond "old" if they remembered seeing the scene at study and "new" if they thought they had not seen the scene. Each scene remained on screen until a response was given, following a 500-ms fixation screen. All participants completed a short practice cycle and at least one full study-test cycle (Table S1). Responses were coded as hit (i.e., "old" response to studied scene), miss ("new" response to studied scene), correct rejection ("new" response to foil), or false alarm ("old" response to foil). Recognition accuracy was calculated by subtracting the false alarm rate (number of false alarms out of total number of foils) from the hit rate (number of hits out of total number of studied scenes). Recognition accuracy was calculated for high- and low-complexity scenes separately. Electrophysiological data for studied scenes were analyzed as a function of subsequent memory at test (i.e., hit or miss) (Johnson et al., 2020; Ofen et al., 2019).

2.4. Electrode placement and localization

Platinum macro-electrodes (4 mm diameter, 10 mm intercontact distance) were placed subdurally for extra-operative ECoG monitoring based solely on the clinical needs of each patient. Three-dimensional electrode reconstructions were created by co-registering post-implantation planar x-ray images of the cortical surface with preoperative T1-weighted spoiled gradient echo MRIs. Automatic parcellation of cortical gyri was performed using FreeSurfer software (Desikan et al., 2006) and anatomical labels were assigned to electrode sites (Pieters et al., 2013). Participants were included in this study by artifact-free electrode coverage of the occipital lobe, as determined by review of individual reconstructions and automatic parcellation results. Electrodes were transformed into standard Talairach space for visual representation across all participants (Fig. 1B) using NeuralAct (Kubaneck and Schalk, 2015).

2.5. ECoG data acquisition and preprocessing

ECoG data were acquired using a 192-channel Nihon Kohden Neurofax 1100A Digital System, sampled at 1 kHz. Raw electrophysiology data were filtered with 0.1-Hz high-pass and 300-Hz low-pass finite impulse response filters, and 60-Hz line noise harmonics were removed using discrete Fourier transform. Data traces were demeaned, and the study data were epoched into 4500-ms trials (-1000 to $+3500$ ms from scene onset). Pathological electrodes and electrodes near lesions identified by the clinical teams (Drs. Asano and Auguste) were removed. Electrodes and epochs displaying epileptiform activity or artifactual signal (from poor contact, machine noise, etc.) were then determined based on visual inspection and removed. Each artifact-free electrode was re-referenced to the common average of all artifact-free electrodes. Each study trial was re-inspected after re-referencing and any trials with residual noise were removed. The final data set included 109 occipital electrodes across all participants (mean \pm SD, 5 ± 2 electrodes/participant; range, 1–9).

2.6. Time-frequency analysis

Time-frequency representations of power were calculated using the FieldTrip toolbox (Oostenveld et al., 2011) for MATLAB (MathWorks Inc., Natick, MA). Each 4500-ms study trial was zero-padded to 12,500 ms, and power was calculated between 5 and 15 Hz (1-Hz resolution, 2-Hz bandwidth) using Fast Fourier transforms with adaptive, frequency-dependent sliding windows of five cycles (e.g., 500-ms window at 10 Hz). Time windows were advanced in increments of 50 ms. Power was z-scored on the pre-stimulus baseline via bootstrapping (see below, *Statistical bootstrapping*).

2.7. Instantaneous frequency analysis

Instantaneous alpha frequency was computed using methods and code developed by Cohen (2014). Each 4500-ms study trial was band-pass filtered between 7 and 14 Hz with a zero-phase, plateau-shaped filter with 15% transition zones. The Hilbert transform was used to extract the phase angle time series from the filtered data and instantaneous frequency was computed by taking the temporal derivative of the phase angle time series, scaled to Hz by the sampling rate and 2π . Because noise in the phase angle time series can cause sharp, non-physiological responses in the derivative, the instantaneous frequency was filtered 10 times using a median filter with different window sizes (i.e., 10 equally spaced time windows between 10 and 400 ms). Instantaneous frequency was calculated per-trial as the median of the median-filtered outputs.

3. Statistical analysis

3.1. Statistical bootstrapping

Scene-induced changes in power were quantified in single trials by normalizing the study data (−150 to +3000 ms from scene onset) on the pre-stimulus baseline (−450 to −150 ms from scene onset) using statistical bootstrapping (Flinker et al., 2015; Johnson et al., 2018). Baseline raw values were pooled into a single time series for each electrode and frequency, from which we randomly selected and averaged r data points (r = number of trials in that participant's data). This process was repeated 1000 times to create normal distributions of pre-stimulus baseline data. Study data were z-scored on the pre-stimulus baseline distributions. This procedure adjusts the time-frequency representations to correct for $1/f$ power scaling and reveal changes in power within each frequency induced by the presentation of a scene.

3.2. Linear mixed-effects models

Behavioral and ECoG data were modeled on the group level using linear mixed-effects models (Baayen et al., 2008; Johnson et al., 2018). To model complexity and age effects in behavior, recognition accuracy, study response time (RT), and recognition test RT data were submitted to models with scene complexity (high, low) and age as fixed effects and participants ($n = 24$) as the random effect.

Because of the nature of the recording technique, electrode coverage differed between participants and it is possible that, in addition to left- or right-hemisphere ECoG, coverage of occipital sub-regions (e.g., V1-V3) differed between participants. The use of mixed-effects models with electrodes as nested random effects controls for the possibility of systematic variability in individual electrode coverage, including hemisphere, sub-region, and the number of electrodes analyzed per participant. To model subsequent memory effects in occipital alpha, power data were submitted to models with subsequent memory (hit, miss) as the fixed effect and participants and nested electrodes ($n = 109$) as random effects. To model complexity and age effects in occipital alpha, power and instantaneous frequency data were submitted to models with scene complexity and age as fixed effects, and participants and nested electrodes as random effects. The false discovery rate (FDR) was used to correct for multiple comparisons at the 0.05 level (i.e., FDR-corrected $p < 0.05$).

Analyses of behavioral RT and of alpha power and frequency were conducted separately for subsequent hit and subsequent miss trials, with the exception of direct analyses of subsequent memory effects (i.e., hit vs. miss). We took this approach instead of submitting the data to a complex model to look for an interaction between subsequent memory (hit, miss), complexity (high, low), and age. Because a three-way interaction would be difficult to interpret, we systemically modeled complexity and age effects separately for subsequently recognized (i.e., hit) and forgotten (miss) scenes. Subsequent memory effects on ECoG data were examined to justify separate models for subsequent hit and miss trials.

Analyses were performed using the MATLAB *fitlme.m* function. To compare effects between subsequently recognized and forgotten scenes, effect sizes were calculated for the interaction terms using Cohen's f^2 (Selya et al., 2012), with $f^2 \geq 0.02$, $f^2 \geq 0.15$, and $f^2 \geq 0.35$ representing small, medium, and large effect sizes, respectively (Cohen, 1988).

3.3. Post-hoc linear regression

Significant data points were averaged separately for high- and low-complexity scenes within each participant and submitted for post-hoc analyses with age and recognition accuracy as predictors. We first determined whether significant complexity by age interactions were driven by age-related differences in the encoding of high- or low-complexity scenes, as indexed by a main effect of age. We further

examined whether these age-related differences predicted recognition accuracy, as indexed by an interaction between age and accuracy. A significant age by accuracy interaction indicates that age-related differences in scene encoding are directly relevant to recognition memory behavior. Analyses were performed using the MATLAB *fitlm.m* function.

3.4. Data availability

De-identified raw data are deposited to the NIMH public database (DOI: 10.15154/1519366). Additional data related to the paper may be requested from the authors.

4. Results

4.1. Age-related gains in memory for complex visual scenes

Across all participants, a mean of 0.94 ± 0.07 of high-complexity scenes and 0.94 ± 0.08 of low-complexity scenes were correctly identified as indoor/outdoor at study (Table S1), indicating proficiency at the scene encoding task. Trials with incorrect indoor/outdoor responses were removed, restricting further analyses to trials in which participants attended sufficiently to indicate the correct scene category (Johnson et al., 2018). Of correctly identified scenes, 0.64 ± 0.20 of high-complexity scenes and 0.66 ± 0.17 of low-complexity scenes were later recognized as "old" (i.e., hit rate). Of the scenes used as foils during recognition, 0.26 ± 0.17 of high-complexity scenes and 0.27 ± 0.18 of low-complexity scenes were falsely identified as "old" (false alarm rate). Recognition accuracy (hit rate – false alarm rate) for high-complexity scenes varied across participants from -0.21 to 0.88 (mean \pm SD, 0.38 ± 0.24), and recognition accuracy for low-complexity scenes varied from -0.01 to 0.80 (mean \pm SD, 0.40 ± 0.22). Note that participants with overall recognition accuracy (collapsed across high- and low-complexity scenes) below zero were excluded from all analyses (see *Participants*). Because participants were not informed of the complexity manipulation, the different accuracy ranges reported for high- and low-complexity scenes reflect scene complexity effects in recognition. Linear mixed-effects modeling revealed a main effect of scene complexity ($F_{(1,44)} = 12.22$, $p < 0.002$) and a complexity by age interaction ($F_{(1,44)} = 12.59$, $p < 0.001$) in recognition accuracy (Fig. 2B). Post-hoc linear regression indicated that this interaction was driven by an age-related increase in recognition accuracy for high-complexity scenes ($\beta = 0.36$, $F_{(1,22)} = 3.19$, $p = 0.09$), not low-complexity scenes ($\beta = -0.06$, $F_{(1,22)} = 0.09$, $p = 0.77$), suggesting developmental gains in memory for complex visual scenes.

Participants' RTs on the scene encoding task varied from 773 to 2402 ms (mean \pm SD, 1522 ± 418 ms) for high-complexity scenes and 753 to 2410 ms (1471 ± 376 ms) for low-complexity scenes. RTs on the recognition test varied from 1264 to 4806 ms (2490 ± 1018 ms) for high-complexity scenes and 1346 to 4446 ms (2367 ± 843 ms) for low-complexity scenes. RTs were not significantly related to age, scene complexity, or the interaction of age and complexity for scenes that were later recognized (study, $p > 0.69$; test, $p > 0.08$) or forgotten (study, $p > 0.87$; test, $p > 0.37$).

4.2. Negative alpha subsequent memory effects in complex visual scenes

Scene perception was associated with task-induced occipital power decreases in the broadband alpha range (~7–14 Hz). Decreased alpha power was evident during the first second of viewing of both high- and low-complexity scenes ($z < -2.57$, $p < 0.01$; Fig. 3A–B). Linear mixed-effect modeling revealed negative subsequent memory effects (i.e., hit < miss) throughout the 3000-ms scene perception period for high- but not low-complexity scenes (FDR-corrected $p < 0.05$; Fig. 3C). Alpha power decreases were maximal during the encoding of complex scenes that were subsequently recognized, predicting memory formation. These subsequent memory effects show that occipital alpha is involved

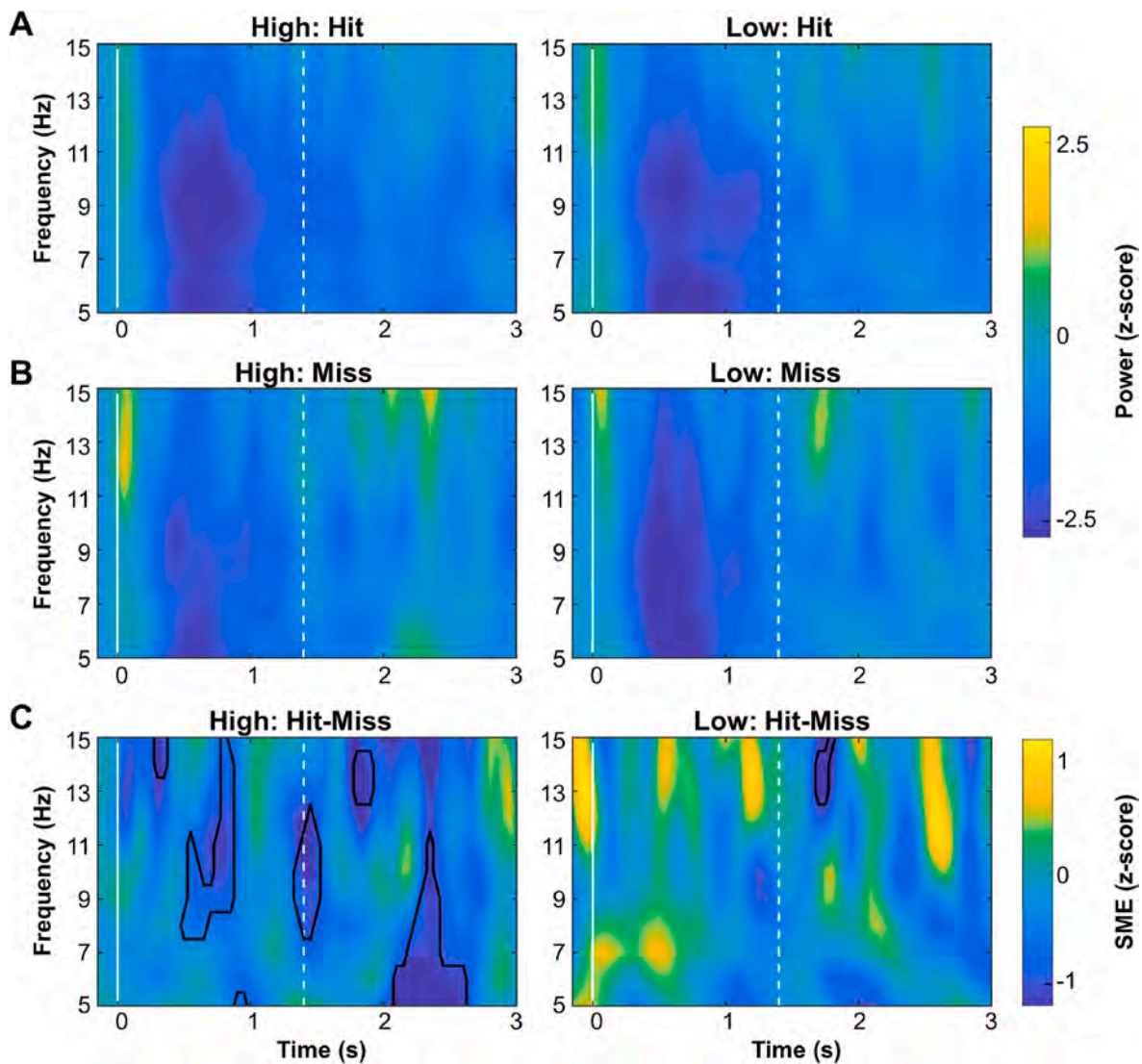


Fig. 3. Negative alpha subsequent memory effects in complex visual scenes. (A) Spectral power (5–15 Hz) for subsequent hit trials during the encoding of high- (left) and low-complexity (right) scenes, averaged across all occipital electrodes for all participants. Scene viewing induced power decreases (i.e., z-scored power values compared with a baseline distribution) in the alpha range ($z < -2.57$, $p < 0.01$). The solid vertical line indicates scene onset and the dashed vertical line indicates mean RT. (B) Same as (A) for subsequent miss trials. (C) Power differences between subsequent hit and miss trials for high- (left) and low-complexity (right) scenes, averaged across all occipital electrodes for all participants. Enclosed areas indicate the data points of significant subsequent memory effects (i.e., hit < miss; FDR-corrected $p < 0.05$). The subsequent memory effects were all negative and mostly specific to high-complexity scenes. The solid vertical line indicates scene onset and the dashed vertical line indicates mean RT. SME, subsequent memory effect.

in the successful encoding of complex visual scenes and demonstrate that decreased alpha power benefits visual memory formation. For this reason, further analyses were performed separately on subsequent hit and miss trials, and relevance to memory is inferred from effects that are specific to the encoding of scenes that were subsequently recognized.

4.3. Age-related decrease in alpha power during complex scene encoding predicts recognition accuracy

To investigate age differences in alpha power during the encoding of subsequently recognized scenes, we conducted linear mixed-effects modeling of alpha power for subsequent hit trials with scene complexity and age as fixed effects. The model revealed significant scene complexity by age interactions during the encoding of subsequently recognized scenes (FDR-corrected $p < 0.05$; mean $f^2 = 0.19$; Fig. 4A). These interactions were maximal between ~7 and 9 Hz and sustained for 400 ms around the indoor/outdoor response (1150–1550 ms from scene onset; RT = 1488 ± 391 ms). Post-hoc linear regression analysis

revealed that these interactions were driven largely by an age-related decrease in power during the encoding of high-complexity scenes ($\beta = -0.31$, $F_{(1,22)} = 2.27$, $p > 0.14$), but not low-complexity scenes ($\beta = 0.09$, $F_{(1,22)} = 0.17$, $p > 0.68$; Fig. 4B). This age-related decrease in power during the encoding of subsequently recognized, high-complexity scenes suggests an age-related increase in visual processing in the occipital cortex during memory formation for high-complexity scenes.

Post-hoc analysis further revealed a significant age by recognition accuracy interaction during the encoding of subsequently recognized, high-complexity scenes ($\beta = -0.31$, $F_{(1,20)} = 4.44$, $p < 0.05$; Fig. 4C, left), suggesting that alpha power is related to age-related gains in the recognition of high complexity scenes. The main effect of accuracy was not significant ($\beta = -0.40$, $F_{(1,20)} = 3.94$, $p > 0.06$). To visualize this interaction, we plotted the relationship between power and accuracy in equally sized subgroups of participants split by median age, referred as children (6.2–13.3 years) and adolescents (13.3–20.5 years). As shown in Fig. 4C (left), lower alpha power predicted greater high-complexity recognition accuracy among adolescents, and this relationship was

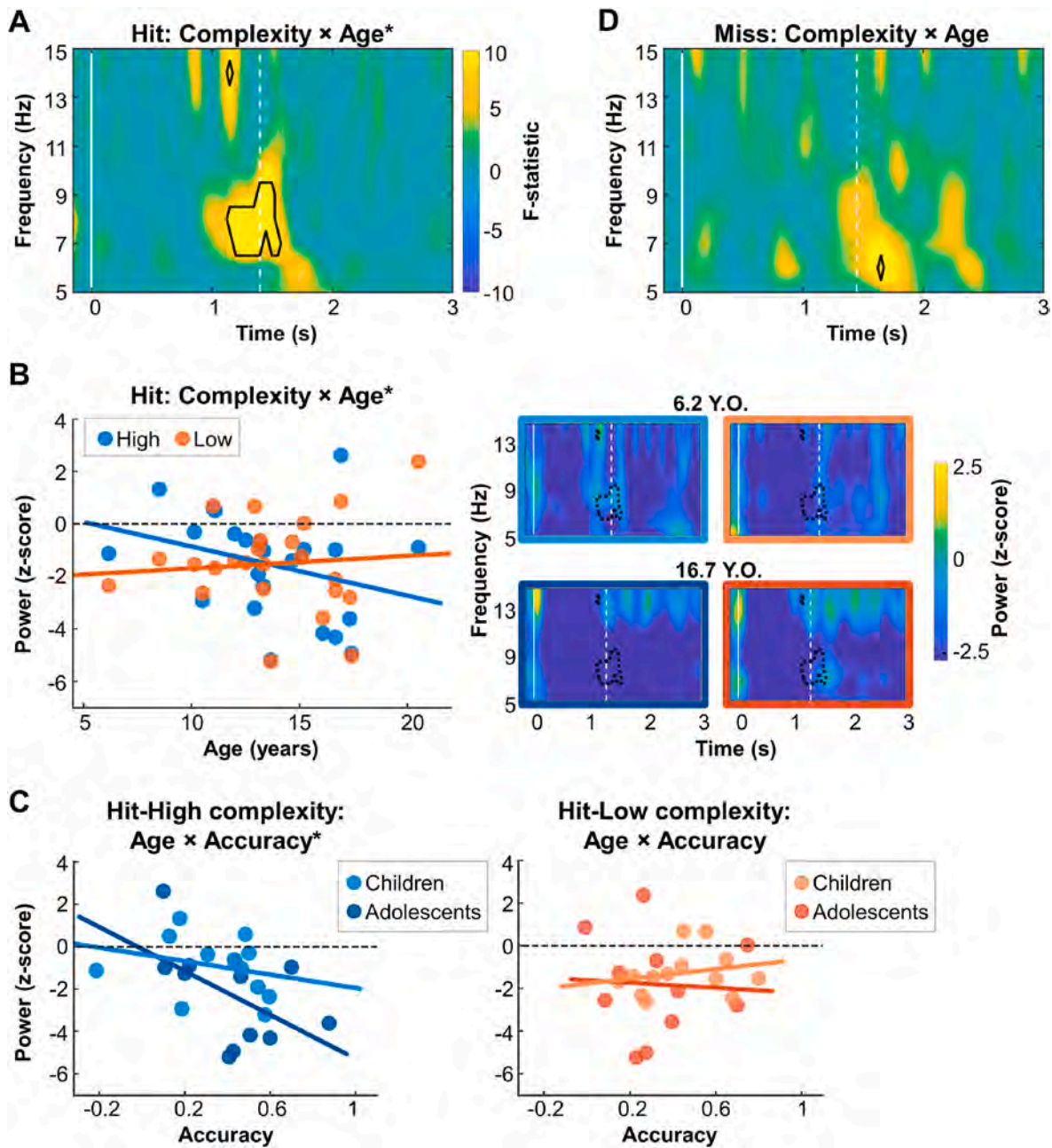


Fig. 4. Age-related decrease in alpha power during complex scene encoding predicts recognition accuracy. (A) F-statistics of complexity by age interactions for subsequent hit trials. Enclosed areas indicate the data points of significant interactions (FDR-corrected $p < 0.05$), which were maximal between ~ 7 and 9 Hz and sustained 400 ms around the indoor/outdoor response (1150–1550 ms from scene onset). The solid vertical line indicates scene onset and the dashed vertical line indicates mean RT. (B) Left: individual alpha power for subsequent hit trials by age, averaged over the data points of significant interactions in (A). The interactions in (A) were largely driven by an age-related decrease in power for high- (blue; $p = 0.15$, $r = -0.31$) but not low- (orange; $p > 0.68$, $r = 0.09$) complexity scenes. Right: representative spectral power for high- and low-complexity subsequent hit trials in two participants aged 6.2 years and 16.7 years demonstrating that age differences differ by scene complexity. Enclosed areas indicate the data points of significant interactions in (A). The solid vertical line indicates scene onset and the dashed vertical line indicates mean RT. (C) Visualization of individual alpha power for high- (right) and low- (left) complexity subsequent hit trials by age and recognition accuracy, averaged over the data points of significant interactions in (A). A significant age by accuracy interaction was identified for high- ($p < 0.05$, left; dark blue, adolescents; light blue, children), but not low- ($p > 0.13$, right; dark orange, adolescents, light orange, children) complexity scenes. Note: Age by accuracy interactions were tested with age as a continuous variable and the median age split is used only for visualization. (D) Same as (A) for subsequent miss trials. Minimal effects observed. (For interpretation of the references to color in this figure legend, the reader is referred to the Web version of this article.)

largely absent among children. In contrast, power during the encoding of low-complexity scenes was not significantly related to recognition accuracy ($\beta = 0.18$, $F_{(1,20)} = 0.12$, $p > 0.73$) or the interaction of age and accuracy ($\beta = -0.50$, $F_{(1,20)} = 2.36$, $p > 0.13$; Fig. 4C, right). By showing that lower occipital alpha power predicted better memory outcomes among adolescents, these results demonstrate that the maturation of

visual processes in the occipital cortex contributes to age-related improvements in the encoding of complex visual scenes (see Fig. 2B).

To assess whether age differences in visual processing are specific to memory formation, we conducted linear mixed-effects modeling for subsequently forgotten scenes (i.e., miss) with complexity and age as fixed effects. We did not observe age-related interactions on miss trials

(mean $f^2 = 0.05$ from the hits mask; Fig. 4D), suggesting that age-related alpha power effects reflect age-related differences in visual memory formation and not visual perception more broadly.

4.4. Age-related increase in instantaneous alpha frequency during complex scene encoding

We observed dynamic changes in alpha frequency during the encoding of both high- and low-complexity scenes (Fig. 5). Linear mixed-effects modeling revealed significant scene complexity by age interactions during the encoding of scenes that were subsequently

recognized (FDR-corrected $p < 0.05$; mean $f^2 = 0.14$; Fig. 5B). These interactions were sustained for 130 ms around the indoor/outdoor response (1220–1350 ms from scene onset; RT = 1488 ± 391 ms). Of note, these interactions were sustained for 347 ms at the uncorrected threshold of $p < 0.05$ (1139–1486 ms from scene onset; mean $f^2 = 0.10$), suggesting that approximately three alpha cycles contributed to the observed effect. These instantaneous frequencies varied from 8.87 to 10.46 Hz (mean ± SD, 9.71 ± 0.44 Hz) during the encoding of high-complexity scenes, and 8.62–10.49 Hz (9.79 ± 0.45 Hz) during the encoding of low-complexity scenes. The window of significant complexity by age interactions in instantaneous frequency overlaps fully

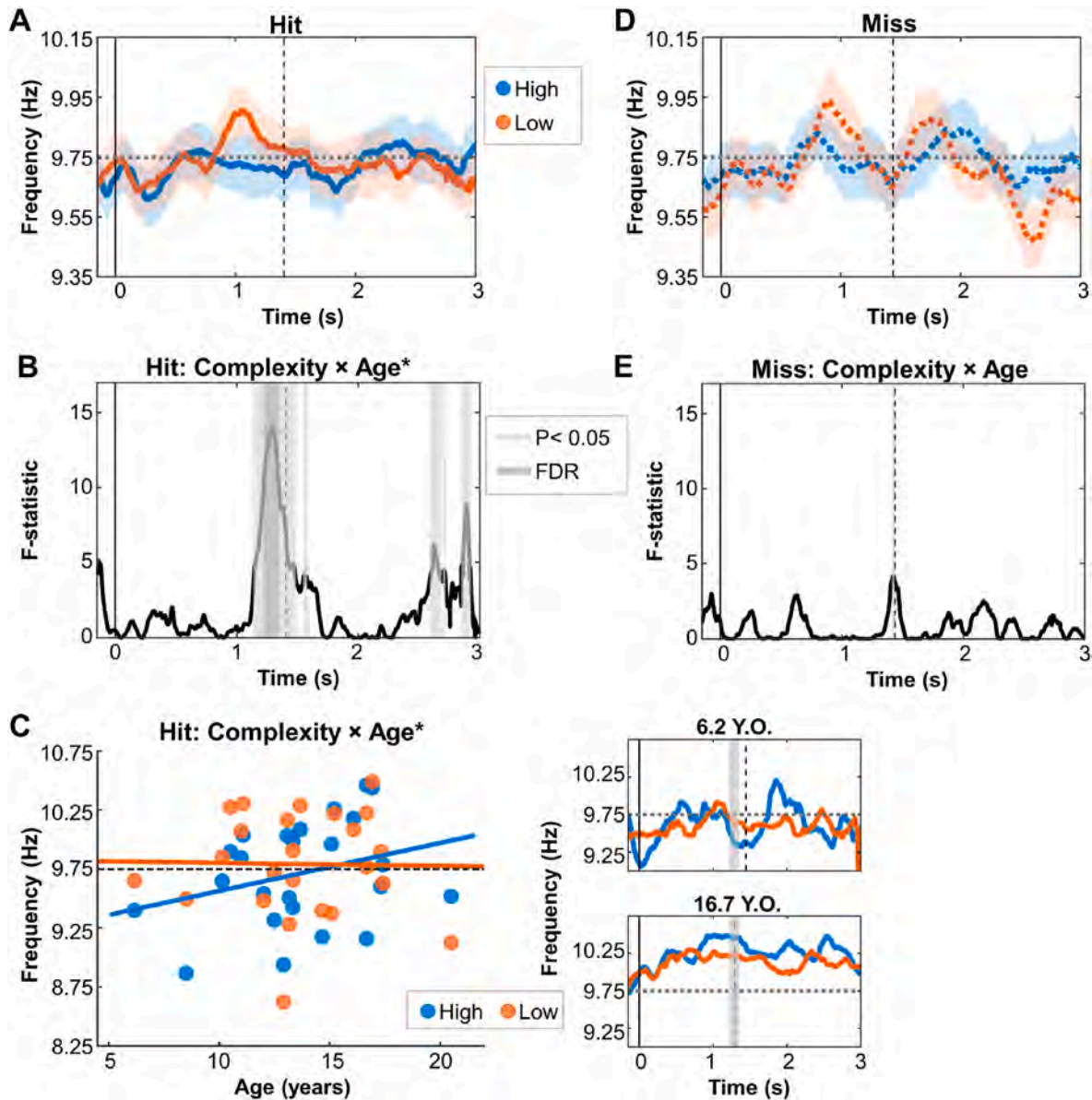


Fig. 5. Age-related increase in instantaneous alpha frequency during the encoding of high-complexity scenes. (A) Instantaneous alpha frequency for high- (blue) and low-complexity (orange) scenes that were subsequently recognized (hit), averaged across all occipital electrodes for all participants. Shaded areas indicate SEM. The solid vertical line indicates scene onset and the dashed vertical line indicates mean RT. (B) F-statistics of complexity by age interactions for subsequent hit trials. Grey shaded areas indicate the epochs of complexity by age interactions. The FDR-corrected interaction was sustained for 130 ms around the indoor/outdoor response (dark grey; 1220–1350 ms from scene onset). The uncorrected interaction (light grey; 1139–1486 ms from scene onset, 347 ms duration) is shown to indicate that approximately three alpha cycles likely contribute to the observed effect. (C) Left: individual instantaneous alpha frequency for subsequently hit trials by age, averaged over the epoch of the FDR-corrected interaction in (B). The interaction was largely driven by an age-related increase in frequency during the encoding of high- (blue; $p > 0.16$, $r = 0.30$) but not low-complexity (orange; $p > 0.93$, $r = -0.02$) scenes. Right: representative instantaneous alpha frequency for high- and low-complexity subsequent hit trials in two participants aged 6.2 years and 16.7 years demonstrating that age differences differ by scene complexity. (D–E) Same as (A–B) for subsequent miss trials. Minimal effects observed. (For interpretation of the references to color in this figure legend, the reader is referred to the Web version of this article.)

in time and partially in frequency with the window of significant complexity by age interactions in alpha power (see Fig. 4A).

Post-hoc analysis indicated that these interactions were driven largely by an age-related increase in instantaneous alpha frequency during the encoding of high-complexity scenes ($\beta = 0.30$, $F_{(1,22)} = 2.10$, $p > 0.16$), but not low-complexity scenes ($\beta = -0.02$, $F_{(1,22)} = 0.01$, $p > 0.93$; Fig. 5C). By showing that adolescents exhibited higher occipital alpha frequency during the processing of complex visual scenes, these results suggest age-related gains in the efficiency of visual processing. However, alpha frequency was not directly related to recognition accuracy (high, $p > 0.74$; low, $p > 0.52$) or to the interaction of age by accuracy (high, $p > 0.81$; low, $p > 0.43$).

We did not observe complexity by age interactions during the encoding of scenes that were subsequently forgotten (mean $f^2 = 0.003$ from the hits mask; Fig. 5D–E). The difference in age-related scene complexity effects between subsequently recognized and forgotten scenes again suggests that age-related effects are specific to visual memory formation and do not reflect general age-related differences in visual perception.

5. Discussion

Using ECoG recordings in children and adolescents, we provide unique evidence showing how the functional maturation of the occipital cortex supports age-related improvements in the formation of memory for complex visual scenes. We first show behaviorally that the recognition of high- but not low-complexity scenes improves with age. This result is consistent with previous work using the same scene subsequent memory task in an independent, non-clinical sample of children and adolescents (Chai et al., 2010). Critically, we then show that individual differences in the recognition of complex scenes are associated with the functional maturation of the occipital cortex, as indexed by complementary measures of alpha power and frequency with millisecond precision. All effects were specific to the encoding of scenes that were subsequently recognized, thus linking the maturation of low-level visual processes to developmental gains in memory for complex visual scenes.

First, we observed task-induced alpha power decreases, or desynchronization, in the first second of viewing both high- and low-complexity scenes. Because alpha desynchronization indexes increased neural activity (Goldman et al., 2002; Haegens et al., 2011; Harvey et al., 2013; van Kerkoerle et al., 2014), this finding indicates visual processing in the occipital cortex during scene perception. Second, we observed negative subsequent memory effects in alpha power during the encoding of high- but not low-complexity scenes. Consistent with findings in adults (Hanslmayr et al., 2016, 2012; Johnson et al., 2020), these negative subsequent memory effects likely reflect increased information processing and suggest that the successful encoding of complex visual scenes places demands on the occipital cortex over and above visual perception.

Third, we observed an age effect in alpha power during the successful encoding of scenes. Specifically, we observed an age-related decrease in alpha power during the successful encoding of high- but not low-complexity scenes. This effect fits nicely with the age-related increase in recognition accuracy observed for high- but not low-complexity scenes. Furthermore, this age-related decrease in alpha power predicted age-related gains in recognition memory performance. During the successful encoding of high-complexity scenes, lower alpha power predicted better recognition in adolescents. No such relationship was observed during the encoding of low-complexity scenes. Together, these results suggest that the functional maturation of the occipital cortex contributes to age-related gains in memory for complex visual scenes, extending the link between the maturation of visual processes and development of visual memory (Chai et al., 2010; Golarai et al., 2010, 2007; Gomez et al., 2017) to low-level visual cortex.

Fourth, we observed an age-related increase in instantaneous alpha frequency during the successful encoding of high- but not low-

complexity scenes. Alpha frequency is associated with rhythmic perception (Samaha and Postle, 2015; VanRullen, 2016) such that particular phases of the alpha cycle are associated with increased neural activity (Haegens et al., 2011; Klimesch et al., 2007) and thus more efficient sensory perception (Busch et al., 2009; Busch and VanRullen, 2010; Mathewson et al., 2009). Because increased alpha frequency indicates more alpha cycles within the same time duration, the age-related increase in frequency suggests increased visual processing efficiency among adolescents compared to children.

The age-related effects observed in complementary measures of alpha power and frequency provide evidence, with millisecond precision, of functional mechanisms supporting prolonged development of visual processing. The evidence presented here is consistent with behavioral evidence of the prolonged development of certain aspects of visual processing (Elleberg et al., 2012; Kovacs et al., 1999; Madrid and Crognale, 2000; Rokszin et al., 2018; Sireteanu; Rieth, 1992; Sloper and Collins, 1998), pointing to possible neuronal mechanisms underlying these behavioral effects. Moreover, this evidence is consistent with neuroimaging and postmortem evidence of prolonged structural maturation of the occipital cortex (Ducharme et al., 2016; Huttenlocher et al., 1982).

Indeed, the age-related differences in alpha power and frequency during the encoding of complex scenes overlapped in time (power: 1150–1550 ms after scene onset, 400 ms duration; frequency: 1220–1350 ms after scene onset, 130 ms duration, FDR-corrected $p < 0.05$; 1139–1486 ms after scene onset, 347 ms duration, uncorrected $p < 0.05$). Furthermore, the instantaneous frequency of the significant interaction (high-complexity: 8.87–10.46 Hz; low-complexity: 8.62–10.49 Hz) overlapped with the upper frequencies of the significant interaction in alpha power (~7–9 Hz). Instantaneous alpha frequency indicates the time-resolved peak oscillatory frequency (Cohen, 2014); therefore, within the overlapping time-frequency window, the age-related increase in alpha frequency may partially explain the age-related decrease in broadband alpha power. This explanation is consistent with previous reports that alpha frequency and amplitude are related through individual amplitude spectra (Nelli et al., 2017) and dually modulated by low-level aspects of visual stimuli (Cohen, 2014). Our results suggest that these complementary measures of alpha power and frequency reflect age-related differences in neural activity contributing to visual memory development.

However, instantaneous alpha frequency was not significantly associated with individual differences in recognition performance. This may be explained by the dissociable, albeit complementary, neural mechanisms reflected in broadband alpha power and peak oscillatory alpha frequency. Whereas instantaneous alpha frequency reflects the timing of neuronal spiking and an oscillatory mechanism that is directly relevant to sensory perception (Cohen, 2014; Haegens et al., 2011; Klimesch et al., 2007; VanRullen, 2016), alpha desynchronization is directly relevant to memory encoding (Hanslmayr et al., 2016, 2012; Johnson et al., 2020). Thus, alpha frequency relates more to visual perception (Samaha and Postle, 2015; Shen et al., 2019; Wutz et al., 2018) than to visual memory performance. Indeed, we showed that alpha desynchronization, but not alpha frequency, was associated with individual differences in memory performance.

In this study, we proposed that the functional maturation of the occipital cortex supports developmental gains in perception and therefore also in memory. The alpha power and frequency effects described above provide strong support for this proposal. Nonetheless, we note limitations of the current study. The first concerns resolution; we investigated effects across occipital electrodes that likely sample different structural and functional occipital sub-regions (e.g., V1–V3) (Wandell et al., 2007). Developmental trajectories may differ by sub-region and some age-related improvements in visual memory likely result from fine-tuned interactions within and across these sub-regions. Future studies may investigate how the functional maturation of different occipital sub-regions contributes to visual memory development. Future

studies may further incorporate structural measures, such as cortical thickness (Ducharme et al., 2016), to investigate how the structural maturation of the occipital cortex gives rise to functional and behavioral developments in visual memory.

Importantly, our findings suggest that age-related effects in occipital alpha activity are relevant to the successful encoding of complex visual scenes, and not simply to visual perception. To this point, we acknowledge that the occipital cortex is one player of many in the brain that contribute to developmental gains in visual memory. Thus, the second limitation concerns neural networks; the prolonged maturation of connections between the occipital cortex and key memory regions, namely, the hippocampus (Poppenk et al., 2013; Poppenk and Moscovitch, 2011) and prefrontal cortex (Barceló et al., 2000; Gazzaley et al., 2007; Zanto et al., 2011) likely contribute to developmental gains in visual memory. Future studies investigating the role of interactions between the occipital cortex and high-level visual and mnemonic regions, as well as regions involved in executive control, may uncover the complex manner by which changes in brain connectivity scaffold cognitive development. Finally, future studies may examine occipital alpha activity during memory retrieval to test the extent to which the perception-induced reactivation of encoded content (Griffiths et al., 2019; Hanslmayr et al., 2016, 2012; Johnson et al., 2020) also supports the development of memory for complex visual scenes.

CRedit author statement

Qin Yin, Elizabeth L. Johnson, Noa Ofen: Conceptualization. Qin Yin, Elizabeth L. Johnson, Noa Ofen: Methodology. Qin Yin, Elizabeth L. Johnson: Software and Formal analysis. Noa Ofen, Eishi Asano, Elizabeth L. Johnson, Kurtis I. Auguste: Investigation. Eishi Asano, Noa Ofen, Kurtis I. Auguste, Robert T. Knight: Resources. Qin Yin, Elizabeth L. Johnson, Lingfei Tang, Kurtis I. Auguste, Eishi Asano, Noa Ofen: Data curation. Qin Yin, Writing - original draft. Qin Yin, Noa Ofen, Elizabeth L. Johnson: Writing - review & editing. Qin Yin, Elizabeth L. Johnson: Visualization. Noa Ofen, Eishi Asano, Robert T. Knight: Supervision. Noa Ofen: Project administration. Noa Ofen: Funding acquisition.

Declaration of competing interest

The authors declare no competing interests.

Acknowledgements

We thank Jessica Damoiseaux, Thomas Fischer, and Zhijian Chen for helpful discussions; and Andrea T. Shafer, Yasuo Nakai, Masaki Sonoda, Naoto Kuroda, and Mohsyn Malik for assistance. This work was supported by the National Institute of Mental Health (R01MH107512 to N. O.), National Institute of Neurological Disorders and Stroke (R01NS64033 to E.A, K99NS115918 to E.L.J., R37NS21135 to R.T.K.), and the Department of Psychology and the Institute of Gerontology at Wayne State University (to N.O and Q.Y.).

Appendix A. Supplementary data

Supplementary data to this article can be found online at <https://doi.org/10.1016/j.neuropsychologia.2020.107625>.

References

- Baayen, R.H., Davidson, D.J., Bates, D.M., 2008. Mixed-effects modeling with crossed random effects for subjects and items. *J. Mem. Lang.* 59, 390–412. <https://doi.org/10.1016/j.jml.2007.12.005>.
- Barceló, F., Suwazono, S., Knight, R.T., 2000. Prefrontal modulation of visual processing in humans. *Nat. Neurosci.* 3, 399–403. <https://doi.org/10.1038/73975>.
- Busch, N.A., Dubois, J., VanRullen, R., 2009. The phase of ongoing EEG oscillations predicts visual perception. *J. Neurosci.* 29, 7869–7876. <https://doi.org/10.1523/JNEUROSCI.0113-09.2009>.

- Busch, N.A., VanRullen, R., 2010. Spontaneous EEG oscillations reveal periodic sampling of visual attention. *Proc. Natl. Acad. Sci. Unit. States Am.* 107, 16048–16053. <https://doi.org/10.1073/pnas.1004801107>.
- Chai, X.J., Ofen, N., Jacobs, L.F., Gabrieli, J.D.E., 2010. Scene complexity: influence on perception, memory, and development in the medial temporal lobe. *Front. Hum. Neurosci.* 4 <https://doi.org/10.3389/fnhum.2010.00021>.
- Clayton, M.S., Yeung, N., Cohen Kadosh, R., 2018. The many characters of visual alpha oscillations. *Eur. J. Neurosci.* 48, 2498–2508. <https://doi.org/10.1111/ejn.13747>.
- Cohen, J., 1988. *Statistical Power Analysis for the Behavioral Sciences*, second. Lawrence Erlbaum Associates, Hillsdale, NJ.
- Cohen, M.X., 2014. Fluctuations in oscillation frequency control spike timing and coordinate neural networks. *J. Neurosci.* 34, 8988–8998. <https://doi.org/10.1523/jneurosci.0261-14.2014>.
- Desikan, R.S., Ségonne, F., Fischl, B., Quinn, B.T., Dickerson, B.C., Blacker, D., et al., 2006. An automated labeling system for subdividing the human cerebral cortex on MRI scans into gyral based regions of interest. *Neuroimage* 31, 698–980. <https://doi.org/10.1016/j.neuroimage.2006.01.021>.
- Ducharme, S., Albaugh, M.D., Nguyen, T.V., Hudziak, J.J., Mateos-Pérez, J.M., Labbe, A., Evans, A.C., Karama, S., Brain Development Cooperative Group, 2016. Trajectories of cortical thickness maturation in normal brain development - the importance of quality control procedures. *Neuroimage* 125, 267–279. <https://doi.org/10.1016/j.neuroimage.2015.10.010>.
- Elleberg, D., Hansen, B.C., Johnson, A., 2012. The developing visual system is not optimally sensitive to the spatial statistics of natural images. *Vision Res* 67, 1–7. <https://doi.org/10.1016/j.visres.2012.06.018>.
- Flinker, A., Korzeniewska, A., Shestuyk, A.Y., Franaszczuk, P.J., Dronkers, N.F., Knight, R.T., Crone, N.E., 2015. Redefining the role of Broca's area in speech. *Proc. Natl. Acad. Sci. Unit. States Am.* 112, 2871–2875. <https://doi.org/10.1073/pnas.1414491112>.
- Gazzaley, A., Rissman, J., Cooney, J., Rutman, A., Seibert, T., Clapp, W., D'Esposito, M., 2007. Functional interactions between prefrontal and visual association cortex contribute to top-down modulation of visual processing. *Cerebr. Cortex* 17, i125–i135. <https://doi.org/10.1093/cercor/bhm113>.
- Golarai, G., Ghahremani, D.G., Whitfield-Gabrieli, S., Reiss, A., Eberhardt, J.L., Gabrieli, J.D.E., Grill-Spector, K., 2007. Differential development of high-level visual cortex correlates with category-specific recognition memory. *Nat. Neurosci.* 10, 512–522. <https://doi.org/10.1038/nn1865>.
- Golarai, G., Liberman, A., Yoon, J.M.D., Grill-Spector, K., 2010. Differential development of the ventral visual cortex extends through adolescence. *Front. Hum. Neurosci.* 3 <https://doi.org/10.1016/j.gloplacha.2016.07.005>.
- Goldman, R.I., Stern, J.M., Engel Jr., J., Cohen, M.S., 2002. Simultaneous EEG and fMRI of the alpha rhythm. *Neuroreport* 13, 2487–2492. <https://doi.org/10.1097/01.wnr.0000047685.08940.d0>.
- Gomez, J., Barnett, M.A., Natu, V., Mezer, A., Palomero-Gallagher, N., Weiner, K.S., Amunts, K., Zilles, K., Grill-Spector, K., 2017. Microstructural Proliferation in human cortex is coupled with the development of face processing. *Science* 355, 68–71. <https://doi.org/10.1126/science.aag0311>.
- Gomez, J., Natu, V., Jeska, B., Barnett, M., Grill-Spector, K., 2018. Development differentially sculpts receptive fields across early and high-level human visual cortex. *Nat. Commun.* 9 <https://doi.org/10.1038/s41467-018-03166-3>.
- Griffiths, B.J., Parish, G., Roux, F., Michelmann, S., van der Plas, M., Kolibius, L.D., Chelvarajah, R., Rollings, D.T., Sawlani, V., Hamer, H., Gollwitzer, S., Kreiselmeyer, G., Staresina, B., Wimber, M., Hanslmayr, S., 2019. Directional coupling of slow and fast hippocampal gamma with neocortical alpha/beta oscillations in human episodic memory. *Proc. Natl. Acad. Sci. Unit. States Am.* 116, 21834–21842. <https://doi.org/10.1073/pnas.1914180116>.
- Haegens, S., Nacher, V., Luna, R., Romo, R., Jensen, O., 2011. α -Oscillations in the monkey sensorimotor network influence discrimination performance by rhythmical inhibition of neuronal spiking. *Proc. Natl. Acad. Sci. Unit. States Am.* 108 <https://doi.org/10.1073/pnas.1117190108>, 19377–19382.
- Hanslmayr, S., Staresina, B.P., Bowman, H., 2016. Oscillations and episodic memory: addressing the synchronization/desynchronization conundrum. *Trends Neurosci.* 39, 16–25. <https://doi.org/10.1016/j.tins.2015.11.004>.
- Hanslmayr, S., Staudigl, T., Fellner, M.-C., 2012. Oscillatory power decreases and long-term memory: the information via desynchronization hypothesis. *Front. Hum. Neurosci.* 6 <https://doi.org/10.3389/fnhum.2012.00074>.
- Harvey, B.M., Vansteensel, M.J., Ferrier, C.H., Petridou, N., Zuiderbaan, W., Aarnoutse, E.J., Bleichner, M.G., Dijkerman, H.C., van Zandvoort, M.J.E., Leijten, F.S.S., Ramsey, N.F., Dumoulin, S.O., 2013. Frequency specific spatial interactions in human electrocorticography: V1 alpha oscillations reflect surround suppression. *Neuroimage* 65, 424–432. <https://doi.org/10.1016/j.neuroimage.2012.10.020>.
- Huttenlocher, P.R., de Courten, C., Garey, L.J., Van der Loos, H., 1982. Synaptogenesis in human visual cortex-evidence for synaptic elimination during normal development. *Neurosci. Lett.* 33, 247–252.
- Johnson, E.L., Kam, J.W.Y., Tzovara, A., Knight, R.T., 2020. Insights into human cognition from intracranial EEG: A review of audition, memory, internal cognition, and causality. *J. Neural Eng.* <https://doi.org/10.1088/1741-2552/abb7a5>. In press.
- Johnson, E.L., Tang, L., Yin, Q., Asano, E., Ofen, N., 2018. Direct brain recordings reveal prefrontal cortex dynamics of memory development. *Sci. Adv.* 4, eaat3702 <https://doi.org/10.1126/sciadv.aat3702>.
- Klimesch, W., Sauseng, P., Hanslmayr, S., 2007. EEG alpha oscillations: the inhibition-timing hypothesis. *Brain Res. Rev.* 53, 63–88. <https://doi.org/10.1016/j.brainresrev.2006.06.003>.
- Kovacs, I., Kozma, P., Feher, A., Benedek, G., 1999. Late maturation of visual spatial integration. *Proc. Natl. Acad. Sci. Unit. States Am.* 96, 12204–12209.

- Kubanek, J., Schalk, G., 2015. NeuralAct: a tool to visualize electrocortical (ECoG) activity on a three-dimensional model of the cortex. *Neuroinformatics* 13, 167–174. <https://doi.org/10.1007/s12021-014-9252-3>.
- Lega, B., Gerami, J., Rugg, M.D., 2017. Modulation of oscillatory power and connectivity in the human posterior cingulate cortex supports the encoding and retrieval of episodic memories. *J. Cognit. Neurosci.* 29, 1415–1432. <https://doi.org/10.1162/jocn>.
- Madrid, M., Crognale, M.A., 2000. Long-term maturation of visual pathways. *Vis. Neurosci.* 17, 831–837. <https://doi.org/10.1017/S0952523800176023>.
- Mathewson, K.E., Gratton, G., Fabiani, M., Beck, D.M., Ro, T., 2009. To see or not to see: prestimulus α phase predicts visual awareness. *J. Neurosci.* 29, 2725–2732. <https://doi.org/10.1523/JNEUROSCI.3963-08.2009>.
- Natu, V.S., Gomez, J., Barnett, M., Jeska, B., Kirilina, E., Jaeger, C., Zhen, Z., Cox, S., Weiner, K.S., Weiskopf, N., Grill-Spector, K., 2019. Apparent thinning of human visual cortex during childhood is associated with myelination. *Proc. Natl. Acad. Sci. Unit. States Am.* 116, 20750–20759. <https://doi.org/10.1073/pnas.1904931116>.
- Nelli, S., Ithipipit, S., Srinivasan, R., Serences, J.T., 2017. Fluctuations in instantaneous frequency predict alpha amplitude during visual perception. *Nat. Commun.* 8 <https://doi.org/10.1038/s41467-017-02176-x>.
- Ofen, N., 2012. The development of neural correlates for memory formation. *Neurosci. Biobehav. Rev.* 36, 1708–1717. <https://doi.org/10.1016/j.neubiorev.2012.02.016>.
- Ofen, N., Kao, Y.-C., Sokol-Hessner, P., Kim, H., Whitfield-Gabrieli, S., Gabrieli, J.D.E., 2007. Development of the declarative memory system in the human brain. *Nat. Neurosci.* 10, 1198–1205. <https://doi.org/10.1038/nn1950>.
- Ofen, N., Tang, L., Yu, Q., Johnson, E.L., 2019. Memory and the developing brain: from description to explanation with innovation in methods. *Dev. Cogn. Neurosci.* 36, 100613 <https://doi.org/10.1016/j.dcn.2018.12.011>.
- Oostenveld, R., Fries, P., Maris, E., Schoffelen, J.M., 2011. FieldTrip: open source software for advanced analysis of MEG, EEG, and invasive electrophysiological data. *Comput. Intell. Neurosci.*, 156869 <https://doi.org/10.1155/2011/156869>.
- Parvizi, J., Kastner, S., 2018. Human intracranial EEG: promises and limitations. *Nat. Neurosci.* 21, 474–483. <https://doi.org/10.1038/s41593-018-0108-2>.
- Peelen, M.V., Glaser, B., Vuilleumier, P., Eliez, S., 2009. Differential development of selectivity for faces and bodies in the fusiform gyrus. *Dev. Sci.* 12, F16–F25. <https://doi.org/10.1111/j.1467-7687.2009.00916.x>.
- Pieters, T.A., Conner, C.R., Tandon, N., 2013. Recursive grid partitioning on a cortical surface model: an optimized technique for the localization of implanted subdural electrodes. *J. Neurosurg.* 118, 1086–1097. <https://doi.org/10.3171/2013.2.JNS121450>.
- Poppenk, J., Evensmoen, H.R., Moscovitch, M., Nadel, L., 2013. Long-axis specialization of the human hippocampus. *Trends Cognit. Sci.* 17, 230–240. <https://doi.org/10.1016/j.tics.2013.03.005>.
- Poppenk, J., Moscovitch, M., 2011. A hippocampal marker of recollection memory ability among healthy young adults: contributions of posterior and anterior segments. *Neuron* 72, 931–937. <https://doi.org/10.1016/j.neuron.2011.10.014>.
- Rokszin, A.A., Györi-Dani, D., Bácsi, J., Nyúl, L.G., Csifcsák, G., 2018. Tracking changes in spatial frequency sensitivity during natural image processing in school age: an event-related potential study. *J. Exp. Child Psychol.* 166, 664–678. <https://doi.org/10.1016/j.jecp.2017.10.004>.
- Russell, B.C., Torralba, A., Murphy, K.P., Freeman, W.T., 2008. LabelMe: a database and web-based tool for image annotation. *Int. J. Comput. Vis.* 77, 157–173. <https://doi.org/10.1007/s11263-007-0090-8>.
- Samaha, J., Postle, B.R., 2015. The speed of alpha-band oscillations predicts the temporal resolution of visual perception. *Curr. Biol.* 25, 2985–2990. <https://doi.org/10.1016/j.cub.2015.10.007>.
- Scherf, K.S., Behrmann, M., Humphreys, K., Luna, B., 2007. Visual category-selectivity for faces, places and objects emerges along different developmental trajectories. *Dev. Sci.* 10, F15–F30. <https://doi.org/10.1111/j.1467-7687.2007.00595.x>.
- Selya, A.S., Rose, J.S., Dierker, L.C., Hedeker, D., Mermelstein, R.J., 2012. A practical guide to calculating Cohen's f^2 , a measure of local effect size, from PROC MIXED. *Front. Psychol.* 3 <https://doi.org/10.3389/fpsyg.2012.00111>.
- Shen, L., Han, B., Chen, L., Chen, Q., 2019. Perceptual inference employs intrinsic alpha frequency to resolve perceptual ambiguity. *PLoS Biol.* 17, e3000025 <https://doi.org/10.1371/journal.pbio.3000025>.
- Sireteane, R., Rieth, C., 1992. Texture segregation in infants and children. *Behav. Brain Res.* 49, 133–139.
- Sloper, J.J., Collins, A.D., 1998. Reduction in binocular enhancement of the visual-evoked potential during development accompanies increasing stereoacuity. *J. Pediatr. Ophthalmol. Strabismus* 35, 154–158.
- Tang, L., Shafer, A.T., Ofen, N., 2018. Prefrontal cortex contributions to the development of memory formation. *Cerebr. Cortex* 28, 3295–3308. <https://doi.org/10.1093/cercor/bhx200>.
- van den Boemen, C., van der Smagt, M.J., Kemner, C., 2012. Keep your eyes on development: the behavioral and neurophysiological development of visual mechanisms underlying form processing. *Front. Psychiatr.* 3 <https://doi.org/10.3389/fpsyg.2012.00016>.
- van Kerkoerle, T., Self, M.W., Dagnino, B., Gariel-Mathis, M.-A., Poort, J., van der Togt, C., Roelfsema, P.R., 2014. Alpha and gamma oscillations characterize feedback and feedforward processing in monkey visual cortex. *Proc. Natl. Acad. Sci. Unit. States Am.* 111, 14332–14341. <https://doi.org/10.1073/pnas.1402773111>.
- VanRullen, R., 2016. Perceptual cycles. *Trends Cognit. Sci.* 20, 723–735. <https://doi.org/10.1016/j.tics.2016.07.006>.
- Wandell, B.A., Dumoulin, S.O., Brewer, A.A., 2007. Visual field maps in human cortex. *Neuron* 56, 366–383. <https://doi.org/10.1016/j.neuron.2007.10.012>.
- Wutz, A., Melcher, D., Samaha, J., 2018. Frequency modulation of neural oscillations according to visual task demands. *Proc. Natl. Acad. Sci. Unit. States Am.* 115, 1346–1351. <https://doi.org/10.1073/pnas.1713318115>.
- Yu, Q., McCall, D.M., Homayouni, R., Tang, L., Chen, Z., Schoff, D., Nishimura, M., Raz, S., Ofen, N., 2018. Age-associated increase in mnemonic strategy use is linked to prefrontal cortex development. *Neuroimage* 181, 162–169. <https://doi.org/10.1016/j.neuroimage.2018.07.008>.
- Zanto, T.P., Rubens, M.T., Thangavel, A., Gazzaley, A., 2011. Causal role of the prefrontal cortex in top-down modulation of visual processing and working memory. *Nat. Neurosci.* 14, 656–661. <https://doi.org/10.1038/nn.2773>.